Journal of Photochemistry & Photobiology, A: Chemistry 415 (2021) 113302

Contents lists available at ScienceDirect

Journal of Photochemistry & Photobiology, A: Chemistry

journal homepage: www.elsevier.com/locate/jphotochem

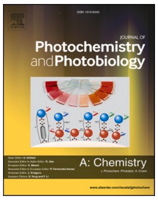

Piperidine based effective chemosensor for Zn(II) with the formation of binuclear Zn complex having specific Al(III) detection ability in aqueous medium and live cell images

Manik Das [a], Biplab Koley [b], Uttam Kumar Das [c], Arijit Bag [d], Soumik Laha [e], Bidhan Chandra Samanta [f], Indranil Choudhuri [g], Nandan Bhattacharyya [g], Tithi Maity [a],*

[a] *Department of Chemistry, Prabhat Kumar College, Contai, Purba Medinipur, West Bengal, 721404, India*
[b] *Department of Chemistry, IIT KGP, Kharagpur, India*
[c] *Depatment of Chemistry, School of Physical Science, Mahatma Gandhi Cental University, Bihar, India*
[d] *School of Natural and Applied Sciences, Maulana Abul Kalam Azad University of Technology, West Bengal, India*
[e] *IICB, Kolkata, West Bengal, India*
[f] *Department of Chemistry, Mugberia Gangadhar Mahavidyalaya, Purbamadinipur, India*
[g] *Department of Biotechnology, Panskura Banamali College, West Bengal, India*

ARTICLE INFO

Keywords:
Sensor
Fluorescence
DFT
Living cell image
Molecular logic gate

ABSTRACT

A schiff base chemosensor **HL** [4-chloro-(((2-(piperidine-1-yl)imino)methyl)phenol], constructed by one step condensation of 2-aminoethyl piperidine and 5- Chloro Salicylaldehyde is illustrated to have its usefulness for selective and sensitive detection of Zn(II) among other metal ions in aqueous solution (HEPES buffer) displaying the colour changes from light blue to turquoise under UV light. The specific detection phenomena of Zn (II) is monitored by the remarkable fluorescence enhancement and notable change in NMR spectral data of fluorescence active **HL** after addition of Zn(II) to it. The impressive high binding constant in 10^6 orders, determined by electronic spectral titration after introduction of Zn(II) to **HL** assure the formation of a Zinc complex during sensing phenomena. In order to check whether the nuclearity of the constructed complex can be increased or not fluorescence enhancement phenomenon is further monitored in presence of different bridging ligands and the results display that only in presence of azide a significant enhancement of Zn(II)-**HL** domain is exposed where as for other bridging ligand the spectra remain unaltered. This observation insists to conduct the reaction between **HL** and $ZnCl_2$ in presence of sodium azide which lead the formation of a Zn complex $[Zn_2(\mathbf{HL})_2(N_3)_4]$ (complex **1**) employing azide as the secondary anionic residue instead of bridging. The single crystal structure of the complex unveils the unique protonation of the piperidine N during the crystallization of the dinuclear motif of the complex **1**. Furthermore the Zn complex due to the presence of remarkable luminescence property have been effectively used for selective sensing of Al(III) ion as metalloreceptor in HEPES buffer solution via turn of fluorescence with remarkable fluorescence quenching constant. In aqueous solution, complex **1** induces a 1:2 complex formation with Al(III) ion indicated by Job's plot analysis. The DFT study suggests the formation of bimetal complex during sensing of Al(III) with complex **1** as metalloreceptor. The in vitro cell imaging study gives a authentic hints for in vivo biomedical application of **HL** as a selective and easy Zn(II) sensor. The two step sensing phenomena of **HL** and complex **1** is further established by advanced molecular logic gate formation.

1. Introduction

Since the last few decade the easy and selective detection of physiologically and environmentally concern metal ions with the organic chemosensors have achieved a special attention to the scientific community due to some special advantages like high sensitivity, easy visualization, short response time for detection [1–7] in comparison to the other detection methods like atomic absorption spectrometry, inductively coupled plasma-atomic emission spectrometry (ICPAES) and voltammetry which led to an expensive instrumentation and high

---

* Corresponding author.
E-mail address: titlipkc2008@gmail.com (T. Maity).

https://doi.org/10.1016/j.jphotochem.2021.113302
Received 8 December 2020; Received in revised form 22 March 2021; Accepted 12 April 2021

quantity sample [8–10]. At the same time recently in this chemosensor development research area, a new concept has been launched where metal organic complexes with the capability of taking another metal ion along with impressive photoluminescence property has been utilized for easy and selective detection of metal ions as metelloreceptor [11–13]. Ru(II)/Re(I)/Ir(III)/Pt(II) based complexes are mainly exposed in this developing area [14–17]. But the design of fluorescence active metalloreceptors based on 3d-metal complexes, particularly Zn(II) complexes, are now in the embryonic stage [18,19].

From biological point of view Zn is a very crucial trace element not only for human body but also for plants and animals [20,21]. It is the second abundant element in human body among different biologically significant metal ions due to its active participation in several biological processes [22–24]. Its deficiency as well as excess accumulation can generate various human health hazards in the form of nausea, vomiting, loss of appetite, stomach cramps, diarrhea, and headaches [25,26]. Beside that over accumulation of this essential metal to the environment as a result of industrial revolution led to some environmental problems which introduce this essential element in a new perspective as 'pollutants'. At the same time after oxygen and silicon aluminum is the third most wide spread (8.3 % by weight) metallic element in the Earth's crust. As a part of life Aluminum stays with us in the form of utensil, building equipment and different packaging items and as a result of which high quantity of free aluminum ions releases Al(III) to the environment, making it toxic [27,28]. In addition the abnormal accumulation of aluminum ion in human body may cause several life threatening diseases like Alzheimer's disease, Parkinson's disease, osteomalacia etc [29–31].

Under this circumstance the selective detection of Zn (II)/Al(III) is very much indispensible for healthy body and environment. As previously discussed the fabrication of effective chemosensors should be the best choice for easy, sensitive and selective detection of Zn(II) and Al (III).

Literature survey exposed several good evidence of individual development of fluorescence active organic probe and metal organic complexes for selective detection Zn(II)/Al(III). As for example, Das et al., [32] Naskar et. al [33], Xu et al. [34], have developed several fluorescence based Schiff base organic chemo sensor for selective detection of Zn(II) and Song et al. [35], have also developed different Zn (II) metalloreceptors for the same purpose. In a parallel way Dwivedi and coworkers [36], Borase and coworkers, [37], Das and coworkers [38], Liu and coworkers [39] have exposed separate organic chemosensor for selective detection of Al(III) but no report has been found to fabricate new metal complex for selective detection of Al(III). All these report highlight the individual construction of either an effective organic probe or metalloreceptor for detection of Zn(II) or Al(III).

Interestingly very few report has been found where organic probe as well as the metalloreceptor, constructed by using mother organic probe, have been used consecutively for the selective detection of Zn(II) and Al (III) respectively. In effective organic probe development area for selective sensing of metal ions Schiff base attracts a special attention. Literature survey also revealed the excellent coordinating power of piperidine based N, N, O donor Schiff base ligand to form metal complexes having different potential application in magnetic field, interaction with macromolecule like DNA, anticancer drug development area etc [40,41]. But very few report where the luminance property of those metal complexes, constructed with this tri dented ligand alone are focused to detect the biologically and environmentally sensitive cations. It is also noticeable that nobody utilizes chloro substituted small easily developing N, N, O donor Schiff base ligand for selective detection of metal ions.

Keeping all these points in mine in the present work one fluorescence active chemosensor **HL**, constructed by one step condensation of 2-aminoethyl piperidine and 5- chloro Salicylaldehyde, have been demonstrated by utilizing its easy and selective sensing behavior to Zn(II). The sensing phenomena are optically and spectroscopically monitored. The electronic titration among **HL** and Zn(II) displays impressively high binding constant providing an idea regarding complex formation. To inspect whether more than one nuclearity complex is obtained or not during sensing, several bridging ligands are introduced to Zn(II)-**HL** adduct and the spectral alteration of fluorescence enhancement is observed. Interestingly in presence of azide anion noticeable spectral change is observed which influence to conduct a reaction among **HL** and $ZnCl_2$ in presence of NaN_3, leading to the formation of a binuclear complex $[Zn_2(\mathbf{HL})_2(N_3)_4]$(complex **1**) with azide as a secondary anionic residue instead of bridging. Consecutively complex **1** have further exposes to detected the physiologically and environmentally concern Al (III) ion as metalloreceptor due to the presence of notable luminescence property. The sensing phenomena of Al(III) is also monitored by adopting the same technique as like Zn(II) sensing. DFT study gives an authentic prove of Zn/Al bimetal complex formation during the sensing of Al(III) with complex **1**.

To get a satisfactory regarding the in vivo biomedical application of **HL** probe for selective detection of Zn(II), living cell image study has been carried out. Furthermore the use of two step advanced logic gate formation represents the sensing process of **HL** and $[Zn_2(\mathbf{HL})_2(N_3)_4]$.

2. Results and discussion

2.1. Synthesis and general characterization of complexes

The Zn complex, $[Zn_2(HL)_2(N_3)_4]$, complex 1 has been synthesized by the reaction of $ZnCl_2$ with the Schiff base ligand (HL) prepared *in situ* via condensation of 2-amino ethyl piperidine and 5-chloro Salicylaldehyde followed by the addition of Sodium azide (Scheme 1). In the initial stage the FTIR spectrum of ligand HL and complex 1 are recorded to get an introductory idea regarding the existence of the bonds (Fig S1 in supplementary information file). For ligand a band at 3521 cm^{-1} is observed which stands for O—H stretching frequency. Within the range of 1730−1740 cm^{-1} the characteristic C═N stretching is observed in HL as well as in complex 1. The sharp bands ranging from 1310 cm^{-1} to 1440 cm^{-1} indicate the vibration of skeleton benzene in both ligand and complex. The UV–vis spectroscopic analysis of the ligand (HL) and complex 1 (Figure S2 in Supporting information file) clarify that two absorption bands are observed at around 325 nm (€ = 9636 M^{-1} cm^{-1}) and 420 nm (€ = 3433 M^{-1} cm^{-1}) in case of ligand (HL). The band cantered at 420 nm may be attributed to the n–π* transition of the azomethine group where as the band at 325 nm arises due to the π-π* transition. The absorption bands in complex 1 shifted toward lower frequencies, 385 (€ = 11,006 M^{-1} cm^{-1}) nm due to CT transition advocating the coordination of azomethine nitrogen and phenolato oxygen with the metal centre.

The electrospray ionization mass spectra (positive mode, *m/z* up to 1200 amu) of the **HL** is recorded in the form of its methanolic solutions (Figure S3 in supporting information file). Ligand **HL** shows one peak at *m/z* 268.4154 amu for species $[\mathbf{HL} + H]^+$ (Figure S3 in the supplementary information file). (Calculated *m/z* = 268.4112 amu) and complex **1** shows one major peak at *m/z* = 407.0526 amu for dinuclear species $[C_{28}H_{38}N_{13}Cl_2O_2Zn_2Na]^{2+}$ (calculated *m/z* = 406.8680 amu (figure S4 in supporting information).

2.2. Crystal structure description

To obtain the solid state structure the single crystal of complex 1 is subjected to SXRD analyses. The crystallographic data and the refinement parameters for complex 1 is given in Table 1.

2.3. $[Zn_2(LH)_2(N_3)_4]$

The X-ray quality single crystals of Zinc complex is crystallized in a centro symmetric *monoclinic* space group '$P2_1/c$' from DMSO/acetonitrile solvent system by slow evaporation at room temperature. The

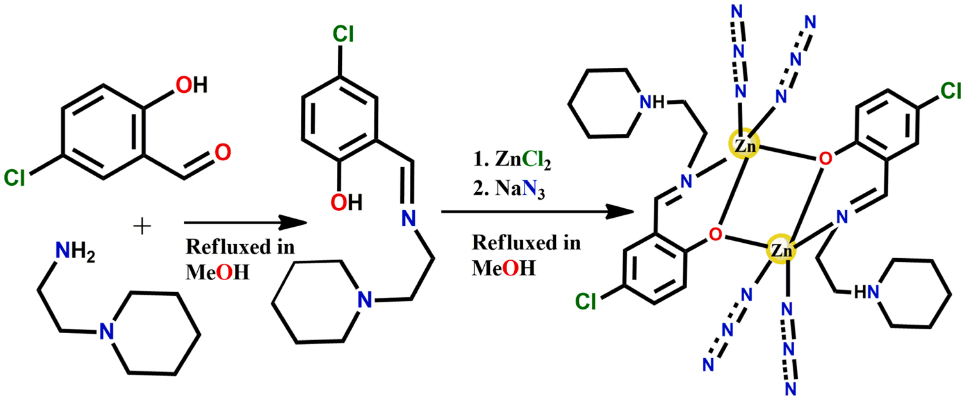

HL

Complex1

Scheme 1. Synthesis of **HL** and complex **1**.

Table 1
The crystallographic data and refinement parameters of Complex 1.

	Complex 1
CCDC No.	2,032,970
Empirical formula	C_{28} H_{38} Cl_2 N_{16} O_2 Zn_2
Formula weight	832.38
Crystal size/mm	0.56 × 0.30 × 0.21
Crystal system	Monoclinic
Space group	$P2_1/c$
a /Å	8.6118(5)
b/Å	25.1200(13)
c /Å	8.6612(5)
$\alpha/^0$	90.00
$\beta/^0$	109.144(2)
$\gamma/^0$	90.00
Volume/$Å^3$	1770.05(17)
Z	2
D_{calc} /gcm^{-3}	1.562
F(000)	856
μ MoKα /mm^{-1}	1.559
Temperature/K	296(2)
R_{int}	0.0306
Range of h, k, l	−7/10, -29/29, -10/10
θ min/max/°	2.632/24.998
Reflections collected/unique/ observed [I>2σ(I)]	15,502 / 3109/ 2818
Data/restraints/ parameters	3109/0/231
Goodness of fit on F^2	1.020
Final R indices [I>2σ(I)]	$R_1 = 0.0257$ $wR_2 = 0.0699$
R indices (all data)	$R_1 = 0.0295$ $wR_2 = 0.0735$

crystal structure of the complex **1** is shown in Fig. 1. The asymmetric unit contains one Zn, one ligand and two azide anions. The oxidation state of zinc is (+2). Although two azide anions and one phenoxide moiety of the ligand coordinate with zinc, but the protonation of the pipyridyl N-atom of the ligand balances the overall charge of the metal (zinc) ion of the complex. The protonation of the pipyridyl N-atom of the ligand was also established from X-ray crystal structure. The protonation further stabilizes the dinuclear unit introducing hydrogen bonding interaction within the structure involving the azide nitrogen atoms. The intra-molecular hydrogen bonding interaction is present between atom **N1** (of pipyridinium moiety) and atom **N3** (of azide) involving **N—H···N** [**N···N** = 2.989; ∠**N—H···N** = 125.78°] interaction of the ligand. The central Zn adopts distorted trigonal bipyramidal geometry (τ ~ 0.78) where two axial positions of the bipyramid are occupied with one oxygen (phenolato) and one nitrogen (imine) atom coming from the ligand backbone and the three basal sites are coordinated with one oxygen (phenolato) and two nitrogen atoms of the added azide residue (Fig. 1). There is strong **C—H··· Π** interactions (3.044 Å) between chlorophenyl ring of one ligand and the hydrogen atom (**H1B**) of the pipyridnium moiety of the other ligand. The **C—H···Π** interactions and overall parallel packing of the metal complex is shown in Fig. 1.

2.4. *Optical and UV–vis spectroscopic signature of ligand HL*

As the synthesized ligand **HL** has potential luminescence property so we initiate our work to examine the sensing ability **HL** in presence of various cations like Co(II), Fe(III), Na(I), Ni(II), Cu(II), Cd(II), Mn(II), Zn (II) and Hg(II) in HEPES buffer medium (pH 7.4). Under UV lamp (λ = 365 nm) a significant luminescence colour change from light blue to turquoise is visualized with naked eye after selective addition of Zn(II) to **HL**(Fig. 2). No such remarkable colour changes are obtained for other analytes. Before work it is prerequisite to check the stability of **HL** in HEPES buffer solution at a fixed pH value 7.4 and the stability is ascertained by means of time–scan UV–Vis experiment (Figure S5 supplementary section). At the same time to resolve the arising question that why the pH has been fixed to 7.4 during the entire works, fluorescence intensity of **HL** and **HL-Zn(II)** adduct at different pH are recorded and the results are summarized in Figure S6. The pictograph revels that **HL-Zn(II)** adduct exhibits highest fluorescence intensity at pH 7.4.

The optical colour changes provide an indication of Zn(II) sensing by **HL**. For further monitoring the selective sensing phenomena of **HL** to Zn (II), in next step the electronic titration is performed among **HL** and Zn (II) in HEPES buffer medium with the measurement of binding constant. Here the alteration of absorbance of **HL** are recorded after incremental addition of Zn(II) to it and the experimental results are summarized in Fig. 3.

The figure clearly display that After addition of incremental concentration of Zn(II) to **HL** according to the expectation the absorbance of **HL** at 328 nm gradually decrease with generation of a new band at 380 nm and two isosbestic points at 275 nm and 345 nm indicating the formation of only one species during titration. The calculated binding constant for **HL**-Zn(II) adduct is found to be 5.44 × 10^6 M^{-1} indicating a Zn(II) complex formation as the ligand has the donar centre to coordinate with the metal centre.

2.5. *^1H NMR spectral titration*

Further, ^1H NMR studies (Fig. 4) in $CDCl_3$ solvent also give a conformational support of the formation of coordination modes of the ligand to Zn(II). The ^1H NMR spectrum of the **HL** exhibits signal at δ 13.25 ppm corresponding to phenolic − OH as expected. Upon addition of 0.5 equiv of $ZnCl_2$ the peak intensity of the phenolic − OH signals decreases considerable and with 1 equiv addition of $ZnCl_2$ the peak intensity of the − OH signal is vanished indicating the formation of Zn

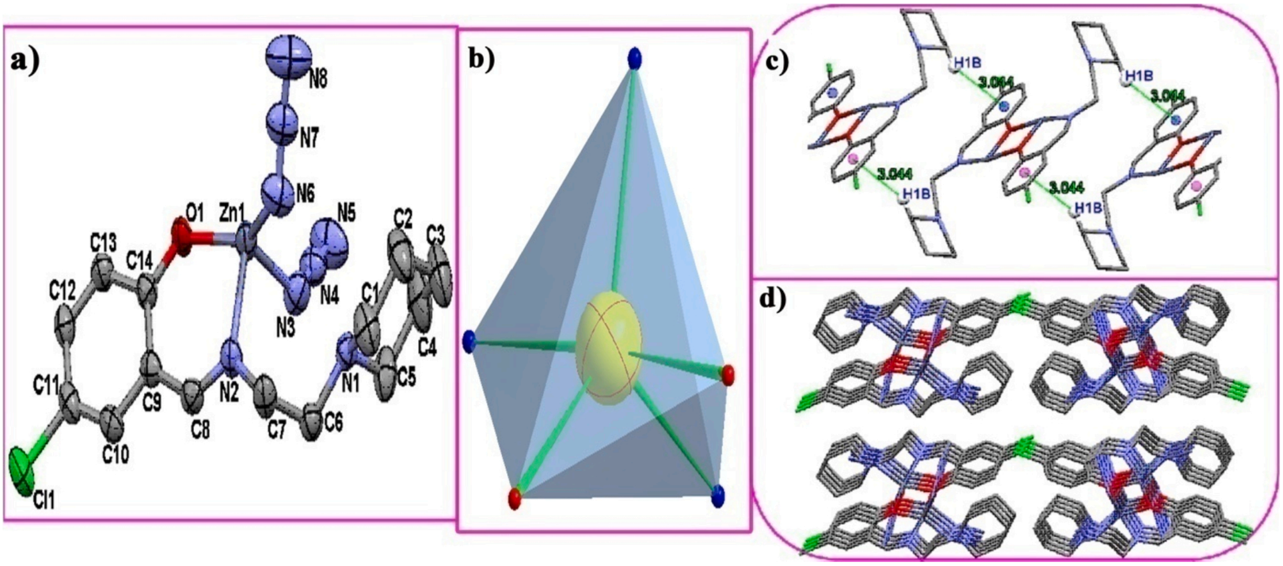

Fig. 1. **a)** Asymmetric Molecular plot of complex **1** **b)** Polyhedron view of central metal ion **c)** the C—H⋯Π interaction present in the crystal (all the H-atom except H1B, azide moieties are hidden for better clarity); **d)** The overall parallel packing of the complex is shown (all the H-atom are hidden for better clarity).

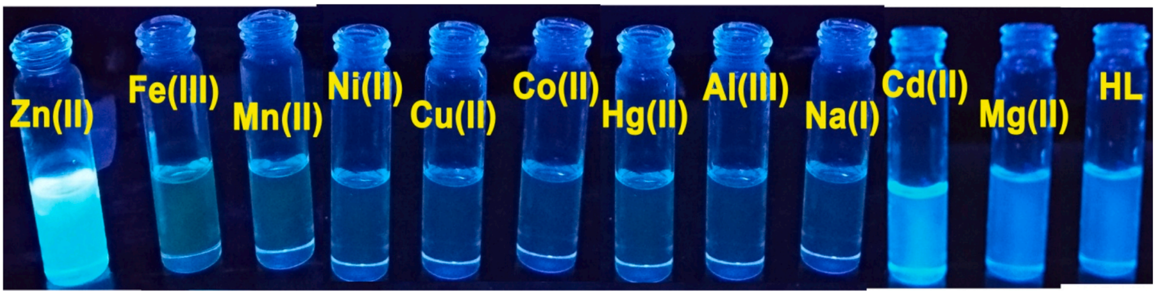

Fig. 2. Under UV the visible colour changes of **HL** after addition of four equivalent of different metal ions separately showing a significant colour changes for Zn(II) in HEPES buffer medium.

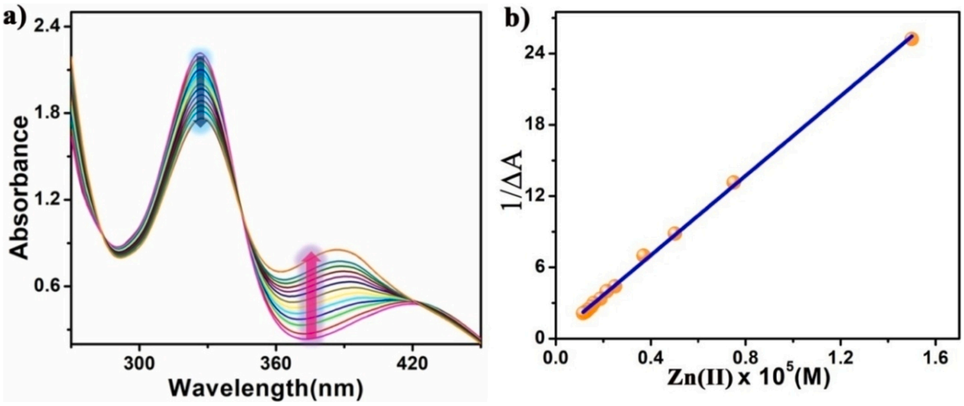

Fig. 3. UV–vis spectral changes of sensor **HL**(0.5×10^{-4}M) in HEPES buffer (pH 7.4) solutions upon addition of Zn(II) ions (0-55 $\times$ 10^{-5}M) (b) Benesi–Hildebrand plot of absorbance titration curve of **HL** with [Zn(II)].

complex with the ligand **HL**. At the same time, the azomethine proton signal shifts to 8.31 ppm from 8.33 ppm. Other aromatic and aliphatic protons display very little shifting. The results at a glance suggest the coordination of one azomethine-N and two phenolate-O of **HL** with Zn (II) to form the Zn complex which is a good support to the obtained structure of the complex **1**.

2.6. Fluorescence study

After fruitful optical, UV and NMR spectral operation in the next level we have moved to investigate the fluorescence intensity change of **HL** after introduction of different metal ions separately to it (Fig. 5 and S7 in supporting information file). The graphical representation displays that the ligand **HL** revels the emission maxima at 492 nm and the remarkable enhancement of fluorescence intensity is visualized only in

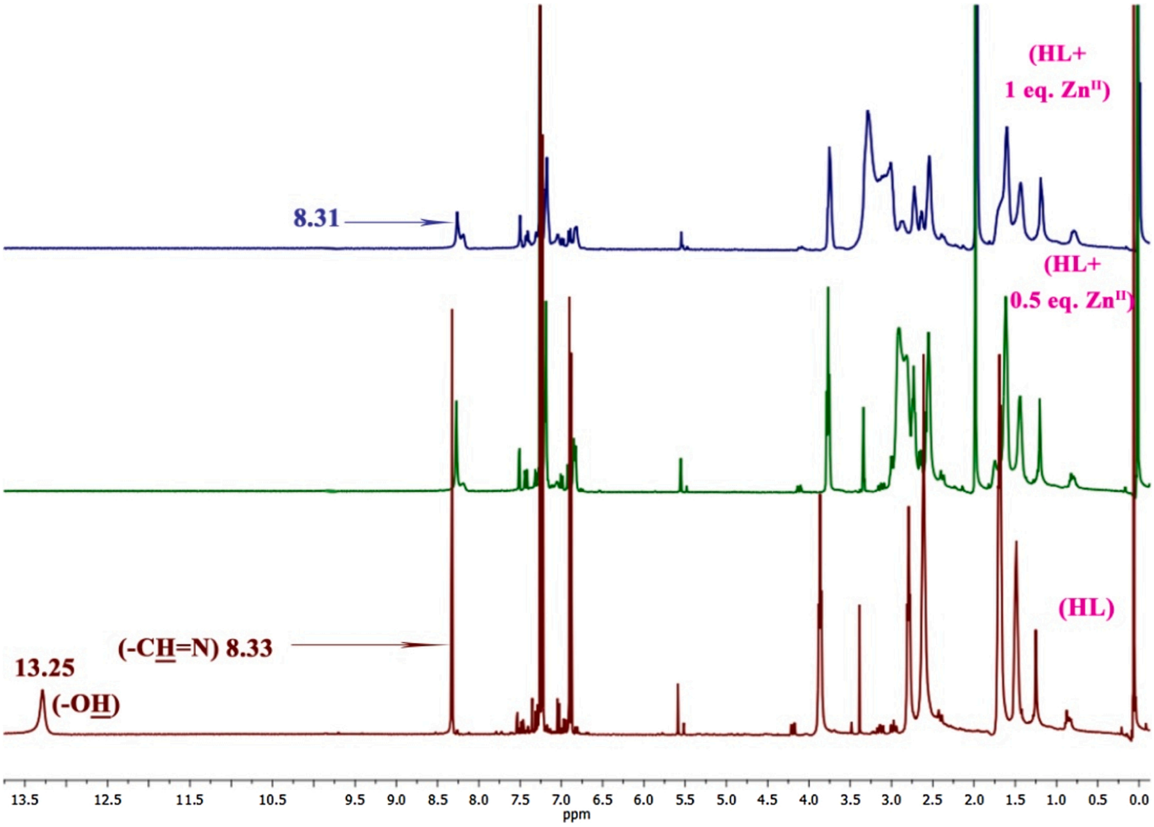

Fig. 4. ^{1}H NMR titration spectra of **HL** in $CDCl_3$ with the absence and presence of $ZnCl_2$.

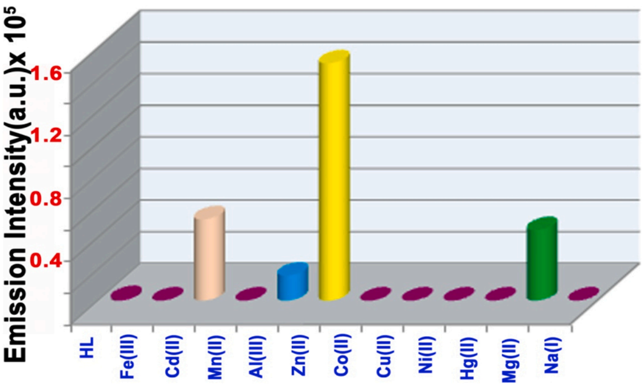

Fig. 5. Fluorescence spectral change **HL** ligand (4×10^{-5} M) at 492 nm in the presence of different cations showing considerable enhancement for Zn(II) ion in HEPES buffer (pH = 7.4) solution.

presence of Zn(II) which is well

Accordance with the introduction of d^{10} system to **HL** showing chelation enhanced fluorescence, CHEF. After coordination, fluorescence emission arises as a result of π-π* ligand-centered charge transfer (LCT) and the role of the zinc ion is to freeze the favorable re-emissive conformation. This is the most probable path way, followed by the ligand **HL** to show strongly emissive power upon zinc coordination. Interestingly the exposure of other analyts towards the spectral change is found to be negligible. Collaterally upon addition of the mixture of all aforementioned metal ions to **HL** (competitive testing) the emission spectra of the ligand nearly do not alter, except on exposure to Zn(II), showing a specific enhancement in the fluorescence intensity and this demonstrate the efficient and selective sensing behaviour of **HL** for Zn (II) over other competitive essential metal ions (fig S8 in supporting information file). To get a quantitative assessment of the relationship between the changes in fluorescence intensity of **HL** with the amount of Zn(II) a detailed fluorometric titration is performed in the same working medium(Fig. 6). The titration result clearly unveils a considerable enhancement of fluorescence intensity at 492 nm with blue shift of 12 nm after incremental addition of Zn(II) to **HL**. The limit of detection (LOD) is found to be 5.34×10^{-8} M, calculate by using the equation DL = K × σ/S, where $K = 3$, σ is the standard deviation of the blank solution and S is the slope of the calibration curves (Fig. 6).

The presence of reversibility is considered to be an important tool in sensing field for practical application. Here the recognition process regarding the presence of reversibility of **HL** is executed by incremental addition of ethylenediaminetetraaceticacid (EDTA) to **HL**-Zn(II) probe and simultaneously the fluorescence intensity is recorded. The titration graph (Fig. 7) depicts that the fluorescence intensity of **HL**-Zn(II) probe at 492 nm gradually decreases after gradual addition of EDTA indicating the demetallation from the receptor along with the recovery of the free receptor for practical application of **HL** as sensor.

In this Zn(II) detection phenomena by chemosensor **HL** the impressive binding constant obtain from electronic titration, abolish of −OH peck, visualized in NMR titration and the amazing enhancement of fluorescence intensity along with shifting of spectral positions give a guaranty regarding the Zn(II) complex formation. During complex formation, to inspect whether the nuclearity of the complex can be increased or not with the help of bridging ligand, the fluorescence intensity changes of **HL**-Zn(II) adduct is further monitored with separate introduction of several bridging ligands to this adduct and the fluorescence intensities are recorded (in Figs. 8 and S9).

2.7. *Response of complex 1 towards Al(III) by fluorescence spectroscopy*

The newly synthesized Zn complex possesses potential luminescent character as perceive from the fluorescence responses. The luminescent

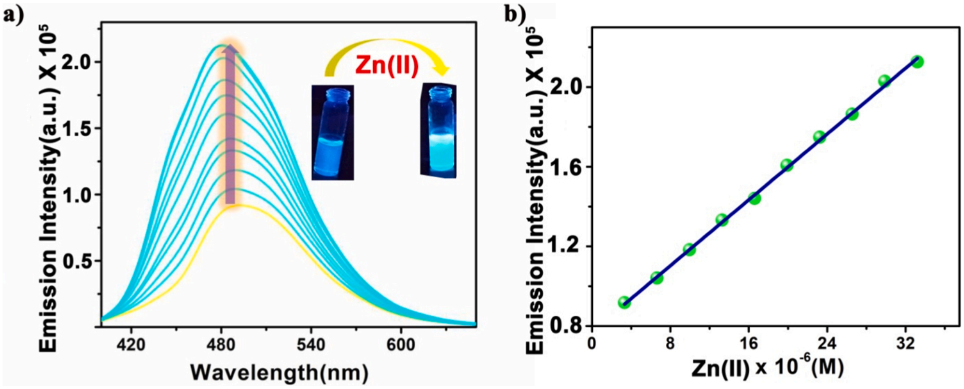

Fig. 6. (a) Impressive fluorescence intensity changes of **HL** (5×10^{-5} M) upon incremental addition of Zn(II) (1.0-12.0 $\times 10^{-5}$ M) in HEPES buffer (pH = 7.4) solution (λex=360 nm, λem=492 nm). Inset: visual colour change observed upon addition of Zn(II) to **HL** solution under UV light (λ = 365 nm) (b) Change of Fluorescence emission intensity of **HL** at 492 nm as a function of Zn(II) concentration for detection limit calculation.

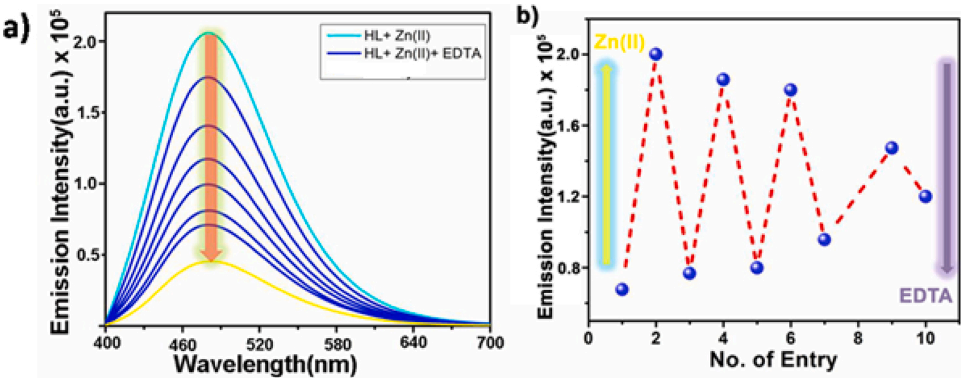

Fig. 7. (a) Fluorescence spectral change of **HL** (30 μM) upon incremental addition of Zn(II) followed by EDTA in HEPES buffer solution at pH 7.4 and (b) The variation of fluorescence intensity at 492 nm after alternative addition of Zn(II) and EDTA to **HL** solution.

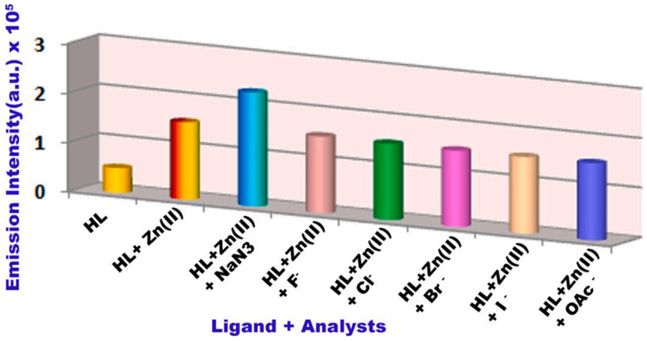

Fig. 8. Change of fluorescence intensity of **HL**-Zn(II) adduct in presence of different bridging ligand (10 μM) showing enhancement of fluorescence intensity in presence of azide.

property of complex **1** is further explore in different solvents namely DMSO, THF, EtOH, MeOH, DMF, DCM and MeCN and the fluorescence intensity change of the complex **1** in different solvents are shown in fig S10 in supporting file.

From the figure one can easily conclude the luminescent property of the complex depends on the nature of the solvents and in DMSO solvent it exhibits its highest fluorescence intensity. At the same time it exhibits a strong emission at 459 nm upon excitation of 370 nm in HEPES buffer medium at pH 7.4. Due to the exposure of photoluminescence property complex **1** can be re-utilized for the second step detection procedure. Keeping this point in mind we further move for the demonstration of complex **1** by utilizing its sensing behavior towards metal ion where it selectively detect Al(III) among several cations like Fe(III), Na(I), Ni(II), Cu(II), Cd(II), Mn(II), Mg(II), Al(III) and Hg(II) in HEPES buffer medium (pH 7.4). This detection phenomenon is optically ascertained along with florescence changes in HEPES buffer medium (Fig S11 in supplementary information file). The fluorometric titration profile of complex **1** (4×10^{-5} M) by Al(III) ($0.3–6 \times 10^{-5}$ M) (Fig. 9) in HEPES buffer solution at pH 7.4 illustrates a rapid diminish of fluorescence intensity after addition of Al(III) to complex **1** with blue shift of 11 nm. The quenching constant value (K_{SV}) is calculated to be 6.7×10^4 M^{-1} using Stern-Volmer equation, $F°/F = K_{SV}[Q] + 1$; where F° and F are the emission intensity in absence and presence of analyte, [Q] is the concentration of the added analyte and K_{SV} is the quenching constant value.

The detection limit of complex **1** for Al(III) ion was found to be 1.64×10^{-8} M (shown in figure S12 in supporting information file). From the quenching constants and detection limit values it can further be conclude that the complex **1** has Potential and selective detection efficacy towards Al(III) ion. The quenching constant values are very much comparable with other Al(III) sensing organic probes [36–38] indicating the strong bonding association between the studied analyte and complex **1**.

2.8. Time resolved fluorescence decay

For understanding the fluorescence quenching mechanism of complex **1** after the addition of Al(III) the time resolved fluorescence decay study have been carried out with the concentration variation of Al(III) in HEPES buffer solution (Table S1 in revised supporting file). The Life time decay profiles of complex **1** in presence and absence of Al(III) are condensed in Fig. 10. The life time fluorescence decay curve of complex

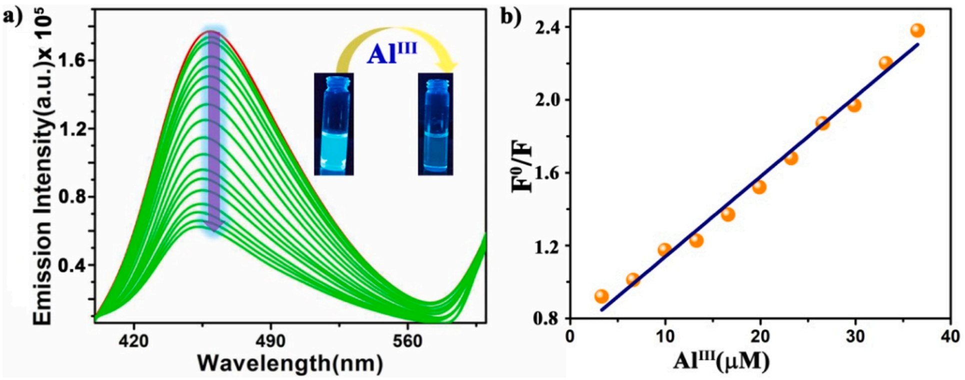

Fig. 9. (a) Alteration of fluorescence spectra of complex **1** (4×10^{-5} M) at 459 nm upon incremental addition of Al(III) solution (0.3-8.0 $\times$ 10^{-5} M) in HEPES buffer (pH = 7.4) solution (λex=360 nm, λem=459 nm). Inset: visual colour change observed with addition of Al(III) to complex **1** solution under UV light (λ = 365 nm) (b) Stern Volmer plot for the detection of quenching constant of complex **1** after addition of Al(III).

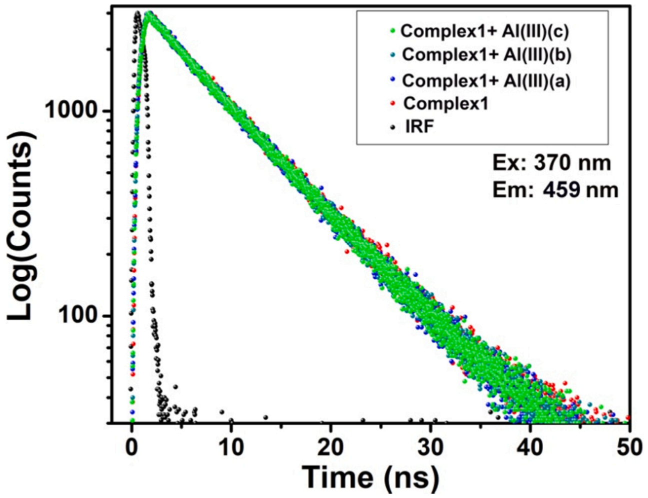

Fig. 10. Time-resolved fluorescence decay of Complex **1** in the absence and presence Al(III) via concentration dependent manner in HEPES buffer.

1 and Complex **1**-Al(III) adduct with variation of Al(III) concentration is fitted by mono exponential function with acceptable value of χ^2. The average life time value (τ^1) for complex **1** is found to be 8.07 ns and upon addition of Al (III) with different concentration to the system no significant changes are visualized. It indicates static quenching mechanism of the complex **1** after addition of Al(III).

2.9. UV vis spectroscopic study

The selective detective phenomena of complex **1** towards Al(III) is further assessed by performing UV–vis spectral titration with the determination of the respective host-guest binding constants value by adopting the same procedure like Zn(II) sensing by **HL**.

Fig. 11 display the titration result. As expected the peak at 382 nm of free complex gradually decreases with the appearance of a new band at 349 nm after addition Al(III). An isosbestic point at 367 appeared on the titration curve indicating the presence of equilibrium which further imply the conversion of the free chemosensor to its bimetal complexes. The binding constant for complex **1** – Al(III) adduct is obtained to be 1.37×10^5 M^{-1}. During sensing of Al(III) by complex **1** the 1:2 ratio determination from the Jobs plot rationalized the fact of Zn/Al bimetal complex formation during sensing (S13 in supporting information file). To optimize the Zn-Al bimetal structure DFT study has been performed.

2.10. DFT calculation for optimization of Zn-Al complex structure

In the foregoing discussion we have successfully explained the selective sensing phenomena of complex **1** towards Al(III) by utilizing several indicating the formation of a single complex during detection. In the next step the structural details of the newly formed complex should be highlighted. The ground state geometry of the complex between complex **1** and Al(III) is optimized with the help of DFT study. From the experiment (JOBS plot) It is seen that during sensing Al(III) can fabricate a complex by maintaining 2:1 stoichiometric ratio and this is an indication regarding the formation of a Zn-Al bimetal complex. The theoretically optimized structure of the Zn-Al complex is exposed in scheme 2 .

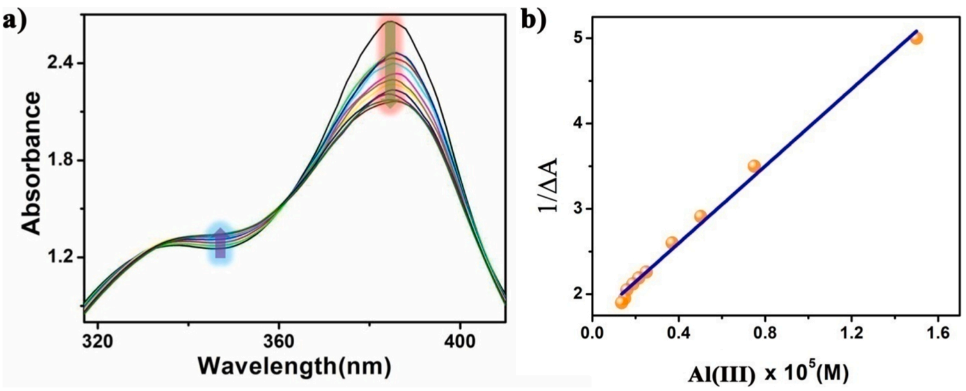

Fig. 11. UV–vis spectral changes of sensor complex **1** (8×10^{-5} M) in HEPES buffer (pH 7.4) solutions upon addition of Al(III) ions (0-16 $\times$ 10^{-5}M) (b) Benesi–Hildebrand plot of absorbance titration curve of Complex **1** with Al(III) for determination of binding constant.

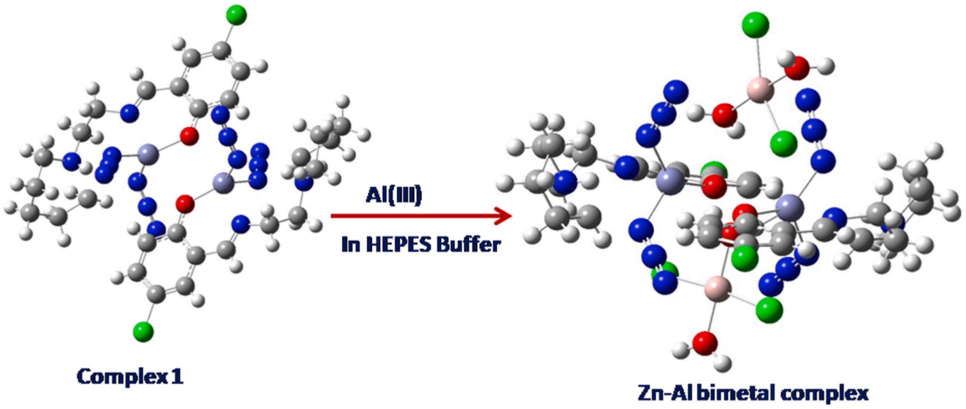

Scheme 2. preparation and structure of Zn/Al bimetal complex during sensing of Al(II) by complex **1.**

The scheme clearly shows that Al(III) holds the centre of an octahedral geometry where two pendent azides of Zn(II) center (complex **1**) act as a bridge among Zn(II) and Al(III)(Zn/Al bimetal complex).

A TDDFT study has been performed in aqueous solvent for complex **1** and newly formed bi metal complex to judge the absorption phenomena and FMO features. By comparing the theoretical and experimental UV–vis spectra of complex **1** one can easily conclude that the complex **1** exist in dimer state. In addition after incorporation Al(III) into complex **1** a significant decreases of energy gap between the HOMO to LUMO is visualized (shown in Fig. 12). As a result of which the absorption maxima shifted to the longer wavelength. It is also observed that the nature of absorption is also different for two different complexes. For complex **1** experimentally two absorbance is noticed centered at 382 nm and 336 nm. Theoretically these two peaks appear at 373 nm (f = 0.01, HOMO→LUMO) and 346 nm (f = 0.1175, HOMO→LUMO+3) which is well fitted with the experimental result. On the other hand after incorporating Al(III) a hypochromism of absorption maxima at 382 nm is observed with red shift and at the same time a new band is appeared at 349 nm which is a good agreement with the theoretical results where two band is seen at 384 nm (f = 0.04, HOMO-2→LUMO+2) and 347 nm (f = 0.0858, HOMO-1→LUMO+3). In Zn complex, electronic transfer takes place from benzene moiety to the hydrocarbon tail whereas in the Zn-Al bi metal complex, electron transfer takes place from the metal moiety to the benzene moiety.

2.11. *Molecular logic gate*

Incremental addition of Zn(II) into the probe **HL** emission intensity enhanced significantly while further introducing micro molar NaN_3 the emission intensity increases impressively. Now Zn(II)-NaN_3 adduct can act as an chemical input (A) into the **HL**. Again ejecting micro molar Al (III) as chemical input (B) into the Zn(II)-NaN_3 adduct fluorescence intensity further quenched. On the basis of this spectral study we forward our direction of this experiment to investigate its use in numerous logic

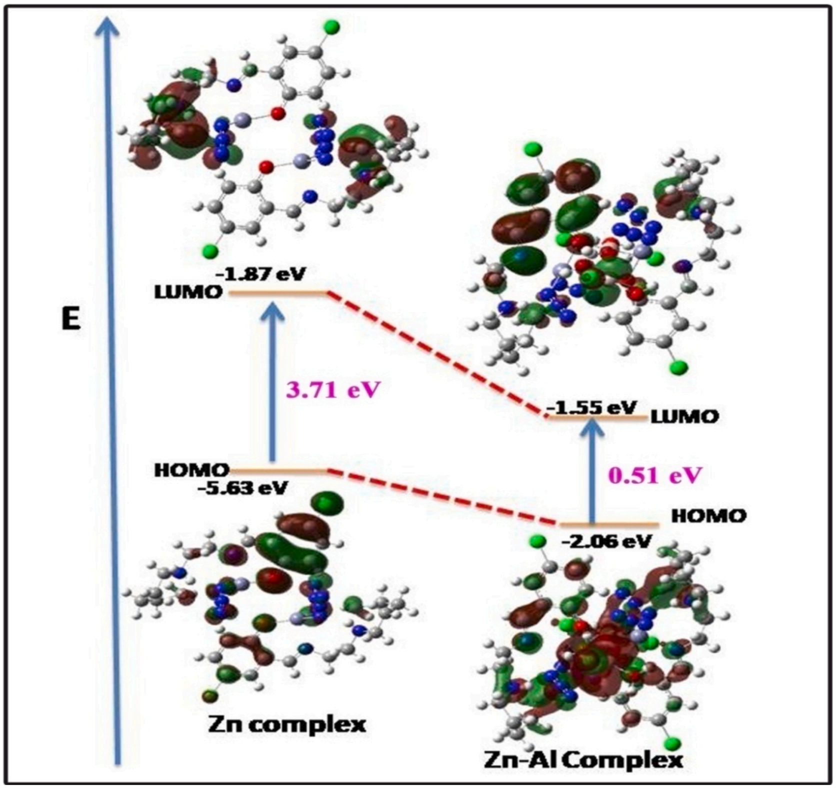

Fig. 12. Frontier orbital involved in complex 1(Zn complex) and Zn/Al bimetal cmplex.

gates by successive addition of inputs such as Zn(II)-NaN_3 adduct and Al (III). This molecular switching behavior of the receptor **HL** towards guest inputs Zn(II)-NaN_3 adduct, Al(III) instigate us to construct a Boolean logic gates and arithmetic calculation at molecular level by monitoring their emission intensity at 459 nm as output. We had investigated this experiment in the manner of emission intensity enhancement for complex only and quenching of emission intensity through sensing Al(III) ignoring emission intensity of the probe because **HL** had a potential emission intensity below the threshold value of the Zn(II) complex, its output assumed as "0″. So to construct a simpler molecular logic device we initiated this experiment from ejection of Zn (II)-NaN_3 adduct into **HL**. We considered Inputs as "1″ for their presence and "0″ for their absence. Outputs are considered as "1″ when the emission intensity is above the certain threshold value (25 % maximum of the complex) and "0″ when it is below the threshold value (Fig. 13a).

When none of the input was introduced to the probe, no characteristic emission intensity was recorded (ignoring the emission intensity of **HL**) indicating output signal "0″ (off state). Addition of the input A Zn (II)-NaN_3 to the probe **HL** fluorescence intensity enhanced indicating output signal "1″ (on state) at 459 nm. Further addition of input B Al (III), no significant enhancement in emission intensity was visualized, so results no output signal. Again in the presence of both inputs simultaneously, no output signal observed denoted as "0″ (off state). It is noticed that **HL** shows the high emission intensity output signal in the manner with addition of input A. It appears to consider the importance of "AND" operation and "NOT" operation with input B. Again when the both inputs are introduced to HL then the output emission intensity value decreases, suggesting the off state as per the truth table (Fig.13b). This combined experiment is an "INHIBIT" logic gate, which consists a particular arrangement of logical functions "AND" and "NOT" (Fig.13c).

2.12. *Molecular memory device*

All the information gathers by adopting the method is well equipped and it can be further congregated through successive logic Circuits. These circuits reserve the following response loop. In this memory device one input is regarded as the "memory element" by considering the output signal as input. The memory device works on a binary logic gate function: either it will be "0″ or "1″ alternatively the two crisp states. The model we have introduce for the advancement of a significant mimicking of the memory element, we take Zn(II)-NaN_3 adduct and Al (III) remarked as the set (S) and reset (R) inputs correspondingly and the photoluminescence was recorded at 459 nm as the output signal (Fig. 14a). When Zn(II)-NaN_3 Adduct acts as input In this memory function, the device recognized the binary state "1″ while under the reset situation Al(III) acts as input, As a result we noticed that the device considered the binary state "0″ (Fig. 14b). So, it can be concluded that we have successfully built a successive logic circuit on the basis of "Write – Read – Erase – Read" property. Hence we can say that by using the same solution of the complex the write – erase cycles could be repeated many times without significant decrease in emission intensity. In the summarization, this system could be properly utilized in technological field. So, by applying molecular successive logic function circuits can be designed which will show a comparable conduct to the logic devices of conventional semiconductors and it can be expected that it be a better technique for construction of molecular microprocessors of integrated circuits.

2.13. *Application of HL for the sensing of Zn (II) in live cell*

In the previous discussion it is already highlighted the favorable binding affinity of **HL** with Zn (II) in HEPES buffer medium via turn on fluorescence. But this achievement applies a force to explore **HL** with respect to the fluorescence imaging of live cell especially for selective detection of intracellular zinc and the fluorescence imaging study has been performed. The images are shown in Fig. 15.

However to materialize these compounds it is prerequisite to check the cytotoxic effect of **HL**, and $ZnCl_2$ on normal cell line(HEK cell)(S14 in supplementary file) as well as in cancer cell line (HeLa)by using MTT assay study in does dependent manner. Up to 100 μM, these two aforementioned materials exhibit no cytotoxicity suggesting the maintenance of the working concentration below 100 μM. The fluorescence microscopic study reveals more or less no fluorescence when the cells are treated with only **HL**. Upon incubation with **HL** followed by $ZnCl_2$ striking switch – ON fluorescence (Fig.15) is appeared inside the cells. Here an intense green fluorescence is observed in the cytoplasmic region but not in the nucleus. Same experiment is done in presence of azide also. But no significant change is visualized in image quality (S15 in supporting file). Before this study in presence of azide, the MTT assay of complex **1** on the two aforementioned cell line is again perform (Fig. S14). Results Show that complex **1** do not exert any adverse cytotoxic effect up to 100 μM concentration The fluorescence microscopic analysis strongly implies that the **HL** can readily cross the membrane barrier, permeate into HEK cells, and rapidly detect intracellular Zn(II). Additionally it is disclose here that the bright field images of treated cells do not expose any gross morphological changes, indicating the cell viability. All these fact open up the avenue for future *in vivo* biomedical applications of the sensor **HL**.

3. Conclusion

From the all above discussion it can be concluded that the

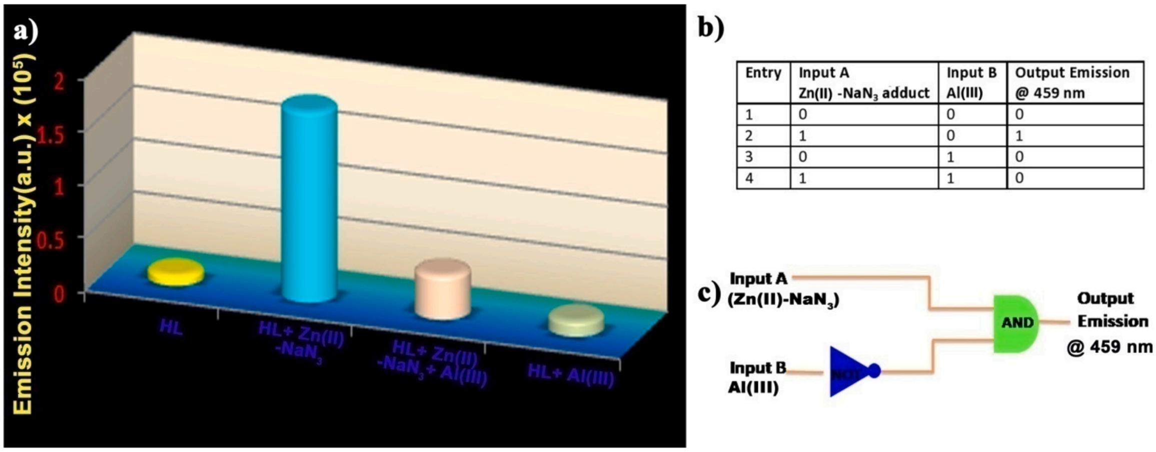

Entry	Input A Zn(II) -NaN_3 adduct	Input B Al(III)	Output Emission @ 459 nm
1	0	0	0
2	1	0	1
3	0	1	0
4	1	1	0

Fig. 13. (a) The emission intensity variation graph of Receptor and Complexes (b) truth table for advance-level molecular logic gate, and (c) circuit diagram of the Complex.

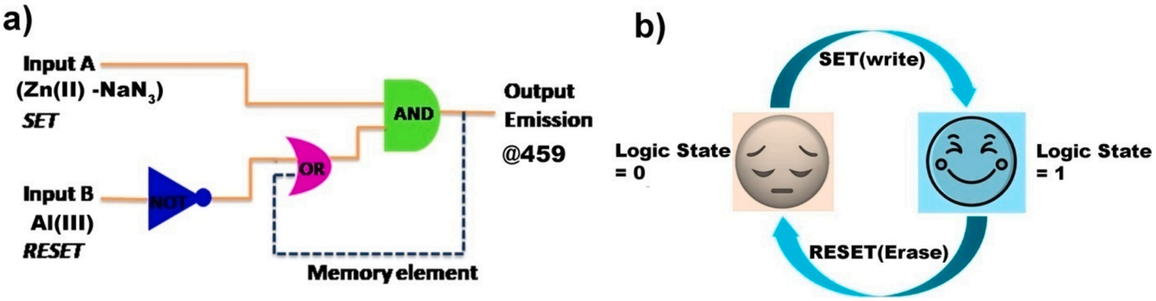

Fig. 14. (a) Consecutive logic circuit of a memory unit and (b) schematic presentation of the reversible logic operation for the memory element with a write – read – erase – read kind of manners.

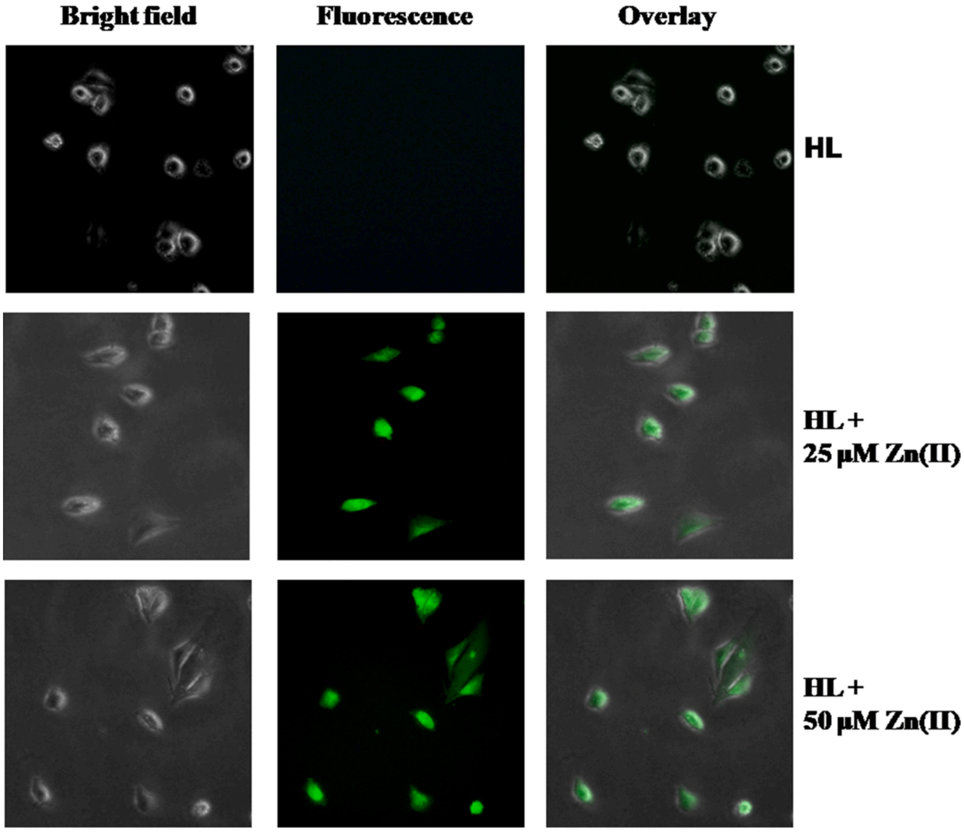

Fig. 15. Fluorescence confocal microscopic images of **HL** probe in presence and absence of Zn(II).

condensation reaction of 5-Chloro salisylaldehyde and 2 amino ethyl piperidine produces a Schiff base chemosensor which can specifically detect Zn(II) among several cations via turn on fluorescence in aqueous solution. The sensing event is further standardized by adopting the electronic and NMR titration methods. The significantly high binding constant value between **HL** and Zn(II), obtain from UV vis spectroscopic titration technique assure the formation of a Zn(II) complex. To get a strong idea whether any higher nuclearity complex can be obtained or not with the help of bridging ligands during sensing, the fluorescence study of **HL**-Zn(II) adduct is further monitor in presence of several bridging ligand. Interestingly in presence of azide a significant alteration of the fluorescence intensity is observed. Getting inspiration from considerable high binding constant among **HL** and Z(II) ion and notable fluorescence changes of **HL**-Zn(II) in presence of azide a reaction is conducted between **HL** and Zn(II) in presence of azide and as a result of which a binuclear zinc complex having azide as secondary anionic residue is produced. According to the hints, getting from fluorescence experiment during sensing of **HL** to Zn(II), complex **1** exhibits an impressively high photo luminance property which helps for further utilization of complex **1** for selective detection of Al(III) among different cations with the formation of Zn/Al bimetal complex whose structure is authenticated by DFT study. Furthermore the two step sensing phenomena is utilized to formulate an INHIBIT logic circuit which is additionally extended to construct a molecular memory device. At last to confirm the biomedical application of **HL** as a sensor the fluorescence microscopic image of HEK cell is taken after incubation with **HL** followed by $ZnCl_2$ and striking switch – ON fluorescence is appeared inside the cells confirming its in vivo use as sensor.

4. Experimental section

4.1. Materials and physical measurements

All the reagents and solvents used in this synthesis were commercially available. Reagent grade chemicals were used in this experiment. So no further purification was needed. 2-aminoethyl piperidine, 5-

chloro Salicylaldehyde, sodiam azide, were procured from Sigma Aldrich Chemicals. $ZnCl_2$ was purchased from Merck. Elemental analyses were performed using a Perkin-Elmer 240C elemental analyzer. For FTIR spectrum data collection ATR mode Bruker Tensor -27 was used. Electronic Absorption spectra were collected using Perkin Elmer UV–vis Lambda 365 spectrophotometer. The fluorescence experiments were performed by using Parkin Elmer Fluorescence spectrometer FL6500.

4.2. *Synthesis of ligand (HL)*

0.1 mL (0.7 mmol) of 2-aminoethyl piperidine was added separately to the methanolic solution of 0.11 g (0.7 mmol) 5- Chloro Salicylaldehyde under sturring condition. After complete addition of the amine to aldehyde (1:1) the resultant solution was refluxed for 3 h. The colour of the solution turned to yellow from colourless. The clear solution was directly used for complex synthesis.

FT-IR (KBr pellet): ν(C═N) 1734 cm^{-1}, ν(O—H) 3456, ν(skeletal vibration) 1440 cm^{-1}, 1540 cm^{-1} ν(Aromatic C—N stretch) 1377 cm^{-1}. UV–vis : 325 nm(π- π*), 420(n- π*).

4.3. *Synthesis of [$Zn_2(HL)_2(N_3)_4$]*

0.095 g (0.7 mmol) $CuCl_2$ was dissolved in methanol (15 mL) and added to 25 mL methanolic solution of **HL_1** ligand (0.248 g, 0.7 mmol) under continuous stirring condition. The resultant solution was then refluxed for additional 3 h. The light yellow coloured solution formed was filtered and from the filtrate single crystals were appeared within three day by slow evaporation. Yield 0.436 g (75 %). *Anal. Calc.*: For $C_{28}H_{38}Cl_2N_{16}O_2Zn_2$ (832.42): C 40.36; H 4.56; N 26.90 % Found: C 40.39; H 4.52; N, 27.10 %., FT-IR data (KBr pellet): ν(C═N) 1705 cm^{-1}, ν(skeletal vibration) 1427 cm^{-1},1310 cm^{-1}.1H NMR [D_6-DMSO, 25 °C]: $\delta = 8.56$(s, 2 H), 7.14−7.58(m, 6 H), 3.10–3.64 (t, 4 H) 2.69–2.91 (m, 12 H), 1.46−1.63(m, 12 H).

Caution! Azides are potentially explosive and should be handled in small amounts and with proper precautions.

4.4. *X-Ray crystallography*

geting the structures of Zn complex single crystal X-ray diffraction (SCXRD) analyses study was carried out using Bruker D8 QUEST diffractometer. The crystallographic data and refinement parameters of the complex were given in Table 1. Reflection data were measured at 296 K, using graphite monochromatic MoK_α radiation with a PHOTON-II detector. The collected data were reduced using the program APEX-III and an empirical absorption correction was carried out using SADABS. [42] The structure was solved using direct methods and refined using the full-matrix least-squares method on F^2 using the WINGX software package. [43,44] The molecular graphics were created using SHELXT [45]. All non-hydrogen atoms were refined with anisotropic parameters. CIF file of complex for the structure reported have been deposited with the Cambridge Crystallographic Data Centre (CCDC). CCDC- 2,032,970, contains the supplementary crystallographic data for the paper. Copies of the data can be obtained, free of charge on application to the CCDC, 12 Union Road, Cambridge, CB2 1EZ UK [Fax: 44 (1233) 336 033 e-mail: deposit@ccdc.cam.ac.uk].

4.5. *Sample preparation for fluorescence and UV spectral study*

The stock solution of ligand **HL** and complex **1** (3×10^{-2} M) was prepared in methanol and DMSO medium respectively and the stock solution of various metal ions (5×10^{-3}M) was prepared in triple distilled water using their perchlorate or chloride salts. For entire fluorescence and absorption studies, in quartz optical cell of 1 cm optical path length appropriate amount of stock solution of **HL** (10^{-2} M) and complex **1** were poured separately to HEPES buffer (pH 7.4) to attain the experimental concentration. After that a required amount of metal ion stock solutions (5×10^{-3} M) were added to it using a micropipette and Spectral data were recorded.

4.6. *Time-resolved fluorescence study*

Lifetime measurement study were carried out with a Horiba JobinYvon Fluorocube-01 NL timecorrelated single photon counting (TCSPC) set up where a picosecond delta diode (DD-

375 L) worked at λex =370 nm and a repetition rate of 1 MHz as excitation source.

4.7. *Computational details*

To understand the Zn/Al bimetal complex formation and reason behind the change of absorption properties the Density Functional Theory (DFT) study using Gaussian 09 [46] package of program have been performed. The structure of complex **1** and Zn-Al bimetal complex have been optimized different complexes to their respective electronic ground states without any symmetry constraints. Optimized structures have been checked by frequency computation. To compute the optical absorbance, Time Dependent DFT (TD-DFT) [47] computation is performed. As the working solvent is HEPES buffer so water solvent is also used in computational study. To include the effect of salvation, continuum polarized model (CPM) [48] is used in all calculations. For DFT calculation, B3LYP [49] functional is used with LANL2DZ basis [50]. LANL2DZ basis which includes the relativistic correction to the basis set is used due to the presence of Zn and Al metal. It is noticed that the B3LYP functional with LANL2DZ basis gives very good results for geometry optimization as well as electronic absorption spectra [51]. In the optimized structure the colour used for the identification of the different atoms are as follows. Dark gray for C, Light gray for H, blue for N, green for Cl, blue gray for Zn(II) and light pink for Al(III)

4.8. *Fluorescence imaging study*

Fluorescent imaging studies were done as per Goswami*et al.*, [52] with modifications. Human embryonic kidney 293 [HEK-293] cells were seeded in a 24 well cell culture plate at a density of 5×10^4 cells per well using Dulbecco’s Modified Eagle’s medium (DMEM) supplemented with 10 % Foetal bovine serum (FBS).Cells were incubated at 37 °C in an atmosphere of air with 5% CO_2.Next day, the cultured media were removed, and cells were washed with phosphate-buffered saline (PBS, pH 7.4) twice. The cells were incubated with ligand **HL** (50 mM) with PBS (pH 7.4) for 10 min, subsequently added $ZnCl_2$ (25/50 mM), and washed with PBS. The cells were observed under a fluorescence microscope (DeWinter) at 400X resolution and captured images using the microscope camera. The images were analyzed using Image J 1.49v software.

The experiment is repeated in presence of presence of azide also.

4.9. *In vitro cytotoxicity assay*

Anti proliferative effect of ligand **HL** and complex **1** on HeLa cell line (human cervical carcinoma cell) were measured by MTT assay. Cells were seeded at a density 2×10^5 cells/well in a 24 well plate. For normal, we used HEK cell line at same concentration. After 24 h of cell seeding, cells were exposed to complex and ligand at different concentration for 24 h. After incubation, cells were washed with 1 X PBS. Thereafter, they were treated with 0.5 mg/mL MTT solution (SRL) and incubated for 3−4 hrs at 37 °C until a purple colour formazan product developed. The resulting product was dissolved in DMSO and OD was measured at 570 nm using a micro plate reader (Biorad). Rate of survival was calculated using following formula. [52,53]

$$\text{Cell viability (\%)} = (\text{OD}_{AT}/\text{OD}_{AC}) \times 100$$

Where OD_{AT}=Absorbency of control cells and OD_{AC}=Absorbency of treated cells.

Declaration of Competing Interest

There are no conflicts to declare.

Acknowledgements

The author are grateful to the Science and Technology Biotechnology, Government of West Bengal for financial assistance through the scheme Gabesanay Bangla with the sanction number 11(sanc.)ST/P/S&T/15G-25/2018 dated: 29.1.2019. Dr. Tithi Maity (T.M.) is thankful to P. K. College, Contai, authority for continuous support to the entire period of work. T.M. is also very much grateful to Dr. Partha Pratim Jana, Assistant Professor, Dept. of Chemistry, IIT Kharagpur for his selfless help for single crystal data collection. The author also would like to express deep gratitude to Prof. Debasis Das, and Miss Somali Mukherjee, Department of Chemistry, University of Calcutta for the valuable scientific suggestion.

Appendix A. Supplementary data

Supplementary material related to this article can be found, in the online version, at doi:https://doi.org/10.1016/j.jphotochem.2021.113302.

References

[1] C.R. Li, S.L. Li, G.G. Wang, Z.Y. Yang, Spectroscopic properties of a chromone-fluorescein conjugate as Mg2+ Bturn on fluorescent probe, J. Photochem. Photobiol. A: Chem. 356 (2016) 700–707.

[2] M.H. Lim, B.A. Wong, W.H. Pitcock, D. Mokshagundam, M.H. Baik, S.J. Lippard, Direct nitric oxide detection in aqueous solution by copper(II) fluorescein complexes, J. Am. Chem. Soc. 128 (2006) 14364–14373.

[3] M. Ghosh, A. Ghosh, S. Ta, J.S. Matalobos, D. ESIPT based Nanomolar Zn2+ sensor for human breast Cancer cell (MCF7) imaging, Chem. Select 2 (2017) 7426–7431.

[4] S. Goswami, A.K. Das, A. Manna, A.K. Maity, H.K. Func, C.K. Quah, P. Saha, A colorimetric and ratiometric fluorescent turn-on fluoride chemodosimeter and application in live cell imaging: high selectivity via specific SiO cleavage in semi aqueous media and prompt recovery of ESIPT along with the X-ray structures, Tetrahedron Lett. 55 (2014) 2633–2638.

[5] D. Udhayakumari, S. Saravanamoorthy, M. Ashok, S. Velmathi Simple imine linked colorimetric and fluorescent receptor for sensing Zn^{2+} ions in aqueous medium based on inhibition of ESIPT mechanism, Tetrahedron Lett. 52 (2011) 4631–4635.

[6] M. Iniya, D. Jeyanthi, K. Krishnaveni, A. Mahes, D. Chellappa Triazole based ratiometric fluorescent probe for Zn2+and its application in bioimaging, Spectrochim. Acta A. Mol. Biomol. Spectrosc. 120 (2014) 40–46.

[7] S.C. Dodani, Q. He, C.J. Chang, A turn-on fluorescent sensor for detecting nickel in living cells, J. Am. Chem. Soc. 131 (2009) 18020–18021.

[8] Y. Liu, P. Liang, L. Guo, Nanometer titanium dioxide immobilized on silica gel as sorbent for preconcentration of metal ions prior to their determination by inductively coupled plasma atomic emission spectrometry, Talanta 68 (2005) 25–30.

[9] A.A. Ensafi, T. Khayamian, A. Benvidi, Determination of copper in whole blood by differential pulse adsorptive stripping voltametry, Anal. Chim. Acta 561 (2006) 225–232.

[10] A.P.S. Gonzales, M.A. Firmino, C.S. Nomura, F.R.P. Rocha, P.V. Oliveira, I. Gaubeur, Peat as a natural solid-phase for copper preconcentration and determination in a multicommuted flow system coupled to flame atomic absorption spectrometry, Anal. Chim. Acta 636 (2009) 198–204.

[11] O. Kotova, S. Comby, T. Gunnlaugsson, Sensing of biologically relevant d-metal ions using a Eu(III)-cyclen based luminescent displacement assay in aqueous pH 7.4 buffered solution, Chem. Commun. 47 (2011) 6810–6812.

[12] S. Pehkonen, Determination of the oxidation-states of iron in natural-waters - a review, Analyst 120 (2011) 2655–2663.

[13] U. Hase, K. Yoshimura, Determination of trace amounts of iron in highly purified water by ion-exchanger phase absorptiometry combined with flow-analysis, Analyst 117 (1992) 1501–1506.

[14] J.N. Demas, B.A. De, Graff, Applications of luminescent transition platinum group metalcomplexes to sensor technology and molecular probes, Coord. Chem. Rev. 211 (2001) 317–351.

[15] V. Guerchais, J. Fillaut Sensory uminescent iridium (III) and platinum (II) complexes for cation recognition, Coord. Chem. Rev. 255 (2011) 2448–2457.

[16] K.K.-W. Lo, M.-W. Louie, K.Y. Zhang, Design of luminecent iridium(III) and rhenium (I) polypyridine complexes as in vitro and in vivo ion molecular and biological probes coord, Chem. Rev. 254n (2010) 2603–2622.

[17] D.-L. Ma, V.P.-Y. Ma, D.S.-H. Chan, K.-H. Leung, H.-Z. He, C.-H. Leung, Recent advances in luminescent heavy metal complex for sensing coord, Chem. Rev. 256 (2012) 3087–3113.

[18] G.-B. Li, H.-C. Fang, Y.-P. Cai, Z.-Y. Zhou, P.K. Thallapally, J. Tian, Construction of a Novel Zn−Ni Trinuclear Schiff Base and a Ni^{2+}Chemosensor, Inorg. Chem 49 (2010) 7241–7243.

[19] M. Aonuma, T. Onodera, S. Morito, A. Wada, T. Akitsu, Sensing of metal ions by hybrid systems of a chiral Schiff base Zn(II) complex and spiropyran, J. Appl. Solution Chem. Model. 2 (2013) 96–104.

[20] N.W. Solomons, Update on zinc biology ann, Nutr. Metab. 62 (2013) 8–17.

[21] V.L. Yang, Zinc and insulin in pancreatic beta-cells, Endocrine 45 (2014) 178–189.

[22] D.D. Mott, M. Benveniste, R.J. Dingledine, pH-dependent inhibition of kainate receptors by zinc, J. Neurosci. 28 (2008) 1659–1671.

[23] E.L. Que, D.W. Domaille, C.J. Chang, Metals in neurobiology: probing their chemistry and biology with molecular imaging, Chem. Rev. 108 (2008) 1517–1549.

[24] A.G. Scrimgeoura, C.H. Stahl, J.P. McClung, L.J. Marchitelli, A.J. Young, Moderate zinc deficiency negatively affects biomechanical properties of rat tibiae independently of body composition, J. Nutr. Biochem. 18 (2007) 813–819.

[25] K.J. Barnham, A.I. Bush, Metals in alzheimer's and parkinson's diseases, Curr. Opin. Chem. Biol. 12 (2008) 222–228.

[26] P. Paoletti, A.M. Vergnano, B. Barbour, M. Casado, Zinc at Glutamatergic Synapses, Neuroscience 158 (2009) 126–136.

[27] W. Barabasz, D. Albińska, M. Jaśkowska, J. Lipiec, Ecotoxicology of aluminum polish, J. Env. Studied 11 (2002) 199–203.

[28] J.R.J. Sorenson, I.R. Campbell, L.B. Tepper, R.D. Lingg, Aluminum in the environment and human health, Environ. Health Perspect. 8 (1974) 3–95.

[29] S. Verstraeten, L. Aimo, P. Oteiza, Aluminium and lade : molecular mechanism of brain, Toxicity Arch. Toxicol. 82 (2008) 789–802.

[30] V. Hornung, F. Bauernfeind, A. Halle, E.O. Samstad, H. Kono, K.L. Rock, K. A. Fitzgerald, E. Latz, Silica crystals and aluminum salts activate the NALP3 inflammasome through phagosomal destabilization, Nat. Immunol. 9 (2008) 847–856.

[31] P.D. Darbre, Aluminium, antiperspirants and breast Cancer, J. Inorg. Biochem. 99 (2005) 1912–1919.

[32] B. Das, A. Jana, A. Das Mahapatra, D. Chattopadhyay, A. Dhara, S. Mabhai, S. Dey, Fluorescein derived Schiff base as fluorimetric zinc (II) sensor via 'turn on' response and its application in live cell imaging, Spectrochim. Acta A. Mol. Biomol. Spectrosc. 212 (2019) 222–231.

[33] B. Naskar, R. Modak, Y. Sikdar, D.K. Maiti, A. Banik, T.K. Dangar, S. Mukhopadhyay, D. Mandal, S. Goswami, A simple Schiff base molecular logic gate for detection of Zn2+ in water and its bio-imaging application in plant system, J. Photochem. Photobiol. A: Chem. 321 (2016) 99–109.

[34] Y. Xu, H. Wang, J. Zhao, X. Yang, M. Pei, G. Zhang, Y. Zhang, L. Lin, A simple fluorescent schiff base for sequential detection of Zn2+ and PPi based on imidazo [2,1-b]thiazole, J. Photochem. Photobiol. A: Chem. 383 (2019) 112026.

[35] H. Song, S. Rajendiran, E. Koo, B.K. Min, S.K. Jeong, T.D. Thangadurai, S. Yoon, Fluorescence enhancement of N2O2-type dipyrrin ligand in two step responding to zinc (II) ion, J. Lumin. 132 (2012) 3089–3092.

[36] R. Dwivedi, D.P. Singh, B.S. Chauhan, S. Srikrishna, A.K. Panday, L.H. Choudhury, V.P. Singh, Intracellular application and logic gate behavior of a 'turn off-on-off' type probe for selective detection of Al3+ and F− ions in pure aqueous medium, Sens. Actuators B Chem. 258 (2018) 881–894.

[37] P.N. Borase, P.B. Thale, S.K. Sahoo, G.S. Shankarling, An "off–on" colorimetric chemosensor for selective detection of Al3+, Cr3+ and Fe3+: its application in molecular logic gate, Sens. Actuators B Chem. 215 (2015) 451–458.

[38] B. Das, S. Dey, G.P. Maiti, A. bhattacharjee, A. Dhara, Atanu Jana, Hydrazinopyrimidine derived novel Al3+ chemosensor: molecular logic gate and biological applications, New J. Chem. 42 (2018) 9424–9435.

[39] H. Liu, T. Liu, J. Li, Y. Zhang, J. Li, J. Song, J. Qu, W. Y. Wong, A simple Schiff base as dual-responsive fluorescent sensor for bioimaging recognition of Zn2+ and Al3+ in living cells, Journal of Materials Chemistry B. doi:10.1039/c8tb01743c.

[40] S. Bhattacharya, S. Sasmal, L. Carrella, E. Rentschler, S. Monhanta, Syntheses, Crystal Structures and Magnetic Properties of a Series of μ-Phenoxo-$\mu_{1,1}$-Carboxylato-$\mu_{1,3}$-Carboxylato Trinickel(II) Compounds, Daltan Trans. 43 (2014) 12065–12076.

[41] S. Sasmal, S. Hazra, P. Kundu, S. Mazumder, N. Aliaga-Alcalde, Eliseo Ruiz, S. Mohanta, Magneto-structural correlation studies and theoretical calculations of a unique family of single end-to-End azide-bridged Ni^{II}_4 cyclic clusters, Inorg. Chem. 49 (2010) 9517–9526.

[42] G.M. Sheldrick, SADABS, Program for Empirical Absorption Correction of Area Detector Data, University of Gottingen, Germany, 1996.

[43] L.J. Farrugia, WINGX—a Windows Program for Crystal Structure Analysis, University of Glasgow, Glasgow, 1998.

[44] L.J. Farrugia, WinGX program for crystallography package, J. Appl. Cryst. 32 (1999) 837–838.

[45] G.M. Sheldrick, SHELX—a Program for Automatic Solution of Crystal Structures, University of Gottingen, Germany, 199.

[46] C. Maurizio, et al., Ab initio study of solvated molecules: a new implementation of the polarizable continuum model, Chem. Phys. Lett. 255 (1996) 327–335.

[47] S. Oliver, M. Reiher, B.A. Hess, Assertion and validation of the performance of the B3LYP* functional for the first transitional metal row and the G2 test set, J. Chem. Phys. 117 (2002) 4729–4737.

[48] C.E. Catherine, et al., Addition of polarization and diffuse functions to the LANL2DZ basis set for P-Block elements, J. Phys. Chem. A 105 (2001) 8111–8116.

[49] A. Bag, P. K.Ghorai, Computational investigation of the ligand field effect to improve the photoacoustic properties of organometallic carbonyl clusters, RSC Adv. 5 (2015) 31575–31583.

[50] A. Bag, P. K.Ghorai, Enhancement of biocompatibility and photoacoustic contrast activity of metal clusters, J. Mol. Graph. Modellin 75 (2017) 220–232.

[51] A. Bag, Application of glucose modified bicyclophosphite derivative of tri-ruthenium carbonyl cluster as advanced photo acoustic contrast agent, Saudi J. Med. Pharm. Sci. 1 (2015) 80–82.

[52] S. Goswami, S. Maity, A.C. Maity, A.K. Das, K. Khanra, T.K. Mandal, N. Bhattacharyya, A macrocyclic piperazine linked extremely Zn2+ selective fluorescent chemosensor with bio-imaging and for H2PO4− sensing, Tetrahedron Lett. 55 (2014) 5993–5997.

[53] W.F. Scherer, J.T. Syverton, G.O. Gey, Studies on the propagation in vitro of poliomyelitis viruses. IV. Viral multiplication in a stable strain of human malignant epithelial cells (strain HeLa) derived from an epidermoid carcinoma of the cervix, J. Exp. Med. 97 (1953) 695–710.